Preparation of Smaller Nine- and Ten-Vertex Monocarbaborane Cages by the Selective Dismantling of Twelve-Vertex Dicarbaboranes *via* the [*nido*-7,9-$C_2B_{10}H_{13}$]$^-$ Anion. Synthesis of the Monocarbaborane Base Adducts *endo*-9-Me-8-(NMe_3)-*arachno*-6-CB_9H_{12}, 9-Me-8-L-*nido*-6-CB_9H_{10} (L = NMe_3, OH^-), and *exo*-6-L-*arachno*-4-CB_8H_{12} (L = SMe_2, NMe_3, Urotropine, Pyridine, Quinoline, MeCN, PPh_3, MeNC)[1a]

Jaromír Plešek,[1b] Bohumil Štíbr,*[,1c,d] Xavier L. R. Fontaine,[1c] Tomáš Jelínek,[1b] Mark Thornton-Pett,*[,1c] Stanislav Heřmánek,[1b] and John D. Kennedy[1c]

Institute of Inorganic Chemistry, Academy of Sciences of the Czech Republic, 250 68 Řež, Czech Republic, and School of Chemistry, University of Leeds, Leeds LS2 9JT, U.K.

Received December 3, 1993®

The *closo*-1,2-$C_2B_{10}H_{12}$ dicarbaborane (**1**) undergoes regiospecific cluster degradation reactions *via* the [*nido*-7,9-$C_2B_{10}H_{13}$]$^-$ anion (**2**) in the presence of Lewis bases L. When L = NMe_3, the reaction is found to proceed *via* carbon-vertex loss to isolate the ten-vertex intermediate *endo*-9-Me-8-(NMe_3)-*arachno*-6-CB_9H_{12} (**3**). Further boron-vertex loss occurs to yield a series of *arachno* nine-vertex compounds *exo*-6-L-4-CB_8H_{12} (**4**) [where L = NMe_3, **4a**; pyridine (py), **4b**; urotropine (uro), **4c**; $^1/_2$ uro, **4d**; and SMe_2, **4e**]. Ligand-exchange reactions between **4e** and stronger Lewis bases, such as py, uro, quinoline (quin), MeCN, PPh_3, and MeNC, afforded compounds **4b–d** and further species of type **4** (where L = quin, **4f**; MeCN, **4g**; PPh_3, **4h**; and MeNC **4i**). These all have clusters that are isostructural with the unsubstituted parent dicarbaborane *arachno*-4,6-$C_2B_7H_{13}$, as documented by X-ray diffraction analysis on **4c**. Crystal data for **4c**: mol wt 251; triclinic; space group $P\bar{1}$; $Z = 4$; $a = 581.78(4)$, $b = 1079.87(6)$, $c = 1181.40(7)$ pm; $\alpha = 105.331(4)$, $\beta = 94.854(4)$, $\gamma = 92.797(4)°$; $U = 0.71127(8)$ nm^3; $R = 0.0423$ and $R_w = 0.0503$ for 2056 reflections with $F_o > 3\sigma(F_o)$. Compound **3** can be oxidized to 9-Me-8-(NMe_3)-*nido*-6-CB_9H_{10} (**5b**) by acetone, and a similar anionic species, [9-Me-8-(HO)-*nido*-6-CB_9H_{10}]$^-$[PPh_4]$^+$ (**5b**), was obtained directly from anion **2** by treatment with acetone. All compounds have been characterized by ^{11}B and ^{1}H NMR spectroscopy, and the unambiguous assignment of the ^{11}B and ^{1}H resonances permits comparisons with the shielding patterns of the structurally related parent analogs such as neutral *arachno*-4,6-$C_2B_7H_{13}$, the anion [*arachno*-6-CB_9H_{14}]$^-$, and the anion [*nido*-6-CB_9H_{12}]$^-$.

Introduction

The pioneering work of Wiesboeck and Hawthorne of over a quarter of a century ago led to the isolation in high yield of the eleven-vertex [*nido*-7,8-$C_2B_9H_{12}$]$^-$ anion *via* boron-vertex loss in a cluster degradation of twelve-vertex *closo*-1,2-$C_2B_{10}H_{12}$ by basic reagents.[2] This constituted the nascence of extensive systematic research into the cluster degradation reactions of carboranes, which subsequently led to the discoveries of families of intermediate-sized dicarbaboranes, such as *closo*-2,3-$C_2B_9H_{11}$, [*nido*-7,9-$C_2B_9H_{12}$]$^-$, the *closo*-$C_2B_8H_{10}$ isomers, *arachno*-4,6-$C_2B_7H_{13}$, *closo*-1,6-$C_2B_7H_9$, and *closo*-1,6-$C_2B_6H_8$, etc., together with their derivatives.[3-5] One of our groups has contributed to these areas of carborane cluster degradation by the isolation of series of unsubstituted parent dicarbaboranes such as [*arachno*-4,5-$C_2B_6H_{11}$]$^-$, [*hypho*-7,8-$C_2B_6H_{13}$]$^-$, *arachno*-4,5-$C_2B_7H_{13}$, *nido*-5,6-$C_2B_8H_{12}$, and *arachno*-6,9-$C_2B_8H_{14}$, as well as the monocarbaboranes *arachno*-4-CB_8H_{14} and *arachno*-4-CB_7H_{13}.[5-7] Recently we have extended these approaches[8] by the use of the twelve-vertex [*nido*-7,9-$C_2B_{10}H_{13}$]$^-$ anion[9] as an alternative starting substrate for the degradative syntheses of the eleven-vertex {*nido*-C_2B_9} and ten-vertex {*nido*-C_2B_8} dicarbaboranes. The solid-state (X-ray)[10] and solution-state (NMR)[8] structures of this interesting [*nido*-7,9-$C_2B_{10}H_{13}$]$^-$ starting anion have only recently been conclusively established.[8,10] Here we now report some further reactions of this anion. These reactions are of importance from the point of view of the strategy of cage degradation because they are associated with the loss of a carbon rather than a boron vertex and lead to monocarbaborane compounds of the ten-vertex {*arachno*-CB_9}, nine-vertex {*arachno*-CB_8}, and eight-vertex {*arachno*-CB_7} cluster types. Some aspects of the reactions have been reported in a preliminary communication,[11] and here we present a more complete account together with some development of the chemistry of the *exo*-6-L-*arachno*-4-CB_8H_{12} system.

* To whom correspondence should be addressed as follows: Crystallographic queries, M.T.-P.; all other queries, B.Š.

® Abstract published in *Advance ACS Abstracts*, June 1, 1994.

(1) (a) Contribution No. 36 from the Anglo-Czech Polyhedral Collaboration (ACPC) between the Institute of Inorganic Chemistry, Czech Academy of Sciences, and the School of Chemistry, University of Leeds. (b) Institute of Inorganic Chemistry. (c) University of Leeds. (d) On leave of absence from the Institute of Inorganic Chemistry.

(2) Wiesboeck, R. A.; Hawthorne, M. F. *J. Am. Chem. Soc.* **1964**, *86*, 1642.

(3) Grimes, R. N. *Carboranes*; Academic: New York, 1970; and references therein.

(4) Onak, T. In *Comprehensive Organometallic Chemistry*; Wilkinson, G., Stone, F. G. A., Abel, E., Eds.; Pergamon: Oxford, U.K., 1982; Chapter 5.4, pp 411–458 and references therein.

(5) Štíbr, B. *Chem. Rev.* **1992**, *92*, 225 and references therein.

(6) Štíbr, B.; Plešek, J.; Heřmánek, S. In *Molecular Structure Energetics, Advances in Boron and the Boranes*; Liebman, J. F., Greenberg, A., Williams, R. E., Eds.; Verlag Chemie: New York, 1988; Chapter 3, pp 35–70 and references therein.

(7) Štíbr, B.; Plešek, J.; Jelínek, T.; Baše, K.; Janoušek, Z.; Heřmánek, S. In *Boron Chemistry, Proceedings of the Second International Meeting on Boron Chemistry*, June 22–26, 1987, Bechyně, Czechoslovakia; Heřmánek, S., Ed.; World Scientific: Singapore, 1987; pp 175–206.

(8) Plešek, J.; Štíbr, B.; Fontaine, X. L. R.; Kennedy, J. D.; Heřmánek, S.; Jelínek, T. *Collect. Czech. Chem. Commun.* **1991**, *56*, 1618.

(9) Dunks, G. B.; Wiersema, R. J.; Hawthorne, M. F. *J. Am. Chem. Soc.* **1973**, *95*, 3174.

(10) Getman, T. D.; Knobler, C. B.; Hawthorne, M. F. *Inorg. Chem.* **1990**, *29*, 158.

(11) Plešek, J.; Jelínek, T.; Štíbr, B.; Heřmánek, S. *J. Chem. Soc., Chem. Commun.* **1988**, 348.

0020-1669/94/1333-2994$04.50/0

Experimental Section

Unless otherwise stated, all reactions were carried out under nitrogen though some operations, e.g. TLC, were carried out in air. All evaporations of solvents were carried out using standard rotary evaporation techniques.

Materials. The $[7,9\text{-}C_2B_{10}H_{13}]^-$ anion ($[NHMe_3H]^+$ salt and Na^+ salt) was prepared by the literature method[8] (from stock solution B). Hexane, dichloromethane, benzene, and toluene were distilled from calcium hydride, and chloroform from P_4O_{10}, prior to use; other chemicals were of reagent or analytical grade and were used as purchased. Column chromatography was performed using silica gel (Lachema 250/100), and preparative TLC was carried out using silica gel (Fluka, type GF 254) as the stationary phase on plates of dimensions 200 × 200 × 1 mm, made on glass formers from aqueous slurries followed by drying in air at 80 °C. The purity of individual chromatographic fractions was checked by analytical TLC on Silufol (silica gel on aluminum foils; detection by diiodine vapor, followed by 2% aqueous $AgNO_3$ spray).

Instrumentation. Proton (^1H NMR) and boron (^{11}B NMR) spectroscopy was performed at 2.35, 4.7, 9.4, and 11.75 T on JEOL FX100, Varian 200, Bruker AM 400, and Varian 500 instruments, respectively. The [^{11}B–^{11}B]-COSY, [^1H–^1H]-COSY, and ^1H–{^{11}B(selective)} NMR experiments were essentially as described in other recent papers from our laboratories.[8,12] Chemical shifts are given in ppm to high-frequency (low field) of Ξ = 32.083 971 MHz (nominally $F_3B{\cdot}OEt_2$ in $CDCl_3$) for ^{11}B (quoted ∓ 0.5 ppm) and Ξ = 100 ($SiMe_4$) for ^1H (quoted ∓0.05 ppm), Ξ being defined as in ref 13. Melting points were measured in sealed capillaries under nitrogen and are uncorrected. Low-resolution mass spectra were obtained using Kratos MS 30 and MEOL HP-5985 instruments (70 eV EI ionization).

***endo*-9-Me-8-(NMe_3)-*arachno*-CB_9H_{12} (3).** The crude and still wet $[NHMe_3]^+[nido\text{-}7,9\text{-}C_2B_{10}H_{13}]^-$ (**2**) (3.08 g; 15 mmol), prepared from the stock solution B (40 mL; 15 mmol) as described in ref 8, was dissolved in ethanol (20 mL) and the solution was treated with 10% aqueous trimethylamine (20 mL) for 1 h at ambient temperature whereupon a white crystalline precipitate separated. This was filtered off, washed with 30% (v/v) aqueous ethanol (20 mL), vacuum-dried (water pump pressure), and dissolved in a minimum amount of benzene (*ca.* 10 mL). Silica gel (*ca.* 5 g) was added to this solution, the benzene was removed, and the residual solid placed onto a dry silica gel column (ca. 2.5 × 30 cm) for chromatography. Elution with benzene removed a small amount of **4a**, while subsequent elution with chloroform gave the main fraction of compound **3** [R_F(anal., $CHCl_3$) 0.40], which was isolated by evaporating the solvent *in vacuo*. Washing with hexane (10 mL) gave white leaflets [2.33 g (76% based on **2** used)] of compound **3**, which was identified as *endo*-9-Me-8-(NMe_3)-*arachno*-6-CB_9H_{12} by NMR spectroscopy as described below. An analytical product, mp 145 °C and m/z(max) 197 ($[^{12}C_5{}^{14}N^{11}B_9{}^1H_{24}]^+$ requires m/z 197), was obtained by crystallization from a dichloromethane solution that was overlayered by an equivalent volume of hexane. Anal. Found: C, 30.51; H, 12.28; B, 48.95; N, 7.22. Calcd for $C_5H_{24}B_9N$: C, 30.69; H, 12.36; B, 49.78; N, 7.16.

***exo*-6-(NMe_3)-*arachno*-4-CB_8H_{12} (4a). (a) From $[NHMe_3]^+[nido\text{-}7,9\text{-}C_2B_{10}H_{13}]^-$ (2).** The crude and still wet $[NHMe_3]^+[nido\text{-}7,9\text{-}C_2B_{10}H_{13}]^-$ (**2**) (3.08 g; 15 mmol), prepared from stock solution B as described in ref 8, was suspended in chloroform (40 mL), and aqueous trimethylamine (10 mL of a 30% aqueous solution) was added over *ca.* 15 min under stirring and cooling to *ca.* 10 °C. The mixture was then stirred for another 3 h at room temperature until all solid had disappeared. The chloroform layer (bottom) was separated off, filtered, and evaporated to dryness. The resulting solid residue was extracted with three 20-mL portions of benzene. The benzene extracts were filtered, silica gel (*ca.* 5 g) was added to the filtrate, and the benzene was then removed by evaporation. The solid residue was placed onto a silica gel column (*ca.* 2.5 × 30 cm) for chromatography. Elution with benzene gave one main fraction [R_F(anal.) = 0.30], which was evaporated, leaving a solid residue. This was washed with hexane (2 × 10 mL) and dried *in vacuo* to give compound **4a** [2.35 g (91%)] as a white solid. An analytical product [mp 155–156 °C, m/z(max) 171 ($[^{12}C_4{}^{14}N^{11}B_8{}^1H_{21}]^+$ requires 171)], identified as *exo*-6-(NMe_3)-*arachno*-4-CB_8H_{12} by NMR spectroscopy, was obtained by crystallization from a dichloromethane solution that was overlayered by an equivalent volume of hexane. Anal. Found: C, 27.94; H, 12.52; B, 50.24; N, 8.13. Calcd for $C_4H_{21}B_8N$: C, 28.29; H, 12.46; B, 50.98; N, 8.25.

(b) From *endo*-9-Me-8-(NMe_3)-*arachno*-6-CB_9H_{12} (3). Compound **3** (50 mg; 256 μmol) was dissolved in chloroform (10 mL), and the solution was treated with ethanol (5 mL) and aqueous trimethylamine (1 mL of a 30% solution) with stirring and cooling at *ca.* 10 °C for 15 min. Stirring was continued for another 2 h at ambient temperature, and the chloroform layer was then separated and evaporated to dryness. The residue was chromatographed by preparative TLC on silica gel in benzene. The main band [R_F(prep) = 0.35] was removed and extracted with dichloromethane, leaving, upon evaporation of the resulting solution, a white product. Crystallization as in the preceding experiment gave 38 mg (87%) of compound **4a**, which was identified by NMR spectroscopy.

***exo*-6-(py)-*arachno*-4-CB_8H_{12} (4b). (a) From $Na^+[nido\text{-}7,9\text{-}C_2B_{10}H_{13}]^-$.** A sample of stock solution B[8] [40 mL, containing 2.52 g (15 mmol) of $Na^+[nido\text{-}7,9\text{-}C_2B_{10}H_{13}]^-$] was allowed to react with pyridine (6 mL) for 4 days at room temperature. The mixture was then evaporated, leaving a thick orange paste which was extracted with chloroform (4 × 20 mL). Silica gel (5 g) was added to the combined chloroform extracts, the chloroform was evaporated, and the solids were placed onto a silica gel column (*ca.* 2.5 × 30 cm) for chromatography. Elution with benzene developed the main orange fraction [R_F(anal.) = 0.41] which was evaporated and dried *in vacuo* to give yellow needles of **4b** [2.4 g (63%)]. An analytical product [m/z(max) 191 ($[^{12}C_6{}^{14}N^{11}B_8{}^1H_{17}]^+$ requires m/z 191), with the most intense fragmentation ions at m/z 185 and 186] was obtained by crystallization from dichloromethane/hexane as in the preceding experiments and identified by NMR spectroscopy.

(b) From *exo*-6-(SMe_2)-*arachno*-4-CB_8H_{12} (4e). Pyridine (2 mL) was added to a solution of **4e** (300 mg; 1.74 mmol) in chloroform (10 mL), and the mixture was heated at reflux for 10 min. The volatile components were then removed by evaporation and the involatile components then separated on a silica gel column (*ca.* 1.5 × 20 cm). Further workup as in the preceding experiment yielded a pure sample of **4b** (250 mg; 76%) which was identified as such by ^{11}B NMR spectroscopy.

***exo*-6-(uro)-*arachno*-4-CB_8H_{12} (4c) and *exo,exo'*-6,6'-(uro)-(*arachno*-4-CB_8H_{12})$_2$ (4d). (a) From $Na^+[nido\text{-}7,9\text{-}C_2B_{10}H_{13}]^-$ (2).** A solution of urotropine (16 g; 114 mmol) and succinic acid (2.36; 20 mmol) in water (100 mL) was added to a sample of stock solution B[8] (60 mL, containing 3.87 g, 23 mmol, of $Na^+[nido\text{-}7,9\text{-}C_2B_{10}H_{13}]^-$), and the mixture was left standing for 3 days at ambient temperature. The white precipitate was filtered off and washed with water (20 mL), diethyl ether (2 × 20 mL), and dichloromethane (3 × 20 mL) to give a white solid compound which was identified as uro·BH_3 by ^{11}B NMR spectroscopy. The filtrate and washings were combined and the organic solvents evaporated. The remaining pasty material was filtered and the solid residue washed with water (2 × 20 mL) and ether (2 × 20 mL) before extraction with dichloromethane (3 × 20 mL). Silica gel (*ca.* 10 g) was added to the dichloromethane extract, the dichloromethane was removed *in vacuo*, and the solids were transferred onto a silica gel column (2.5 × 30 cm) for chromatography. Elution with dichloromethane gave the first fraction [R_F(anal.) = 0.37]. This was reduced in volume to *ca.* 5 mL, overlayered with hexane (*ca.* 15 mL), and left to crystallize for *ca.* 1 week. The resulting needle-shaped white crystals (920 mg; 16%) were identified as *exo,exo'*-6,6'-(uro)-(*arachno*-4-CB_8H_{12})$_2$ (**4d**) [mp 192–193 °C; m/z(max) 364 ($[^{12}C_8{}^{14}N_4{}^{11}B_{16}{}^1H_{36}]^+$ requires m/z 364) with the most intense peak in the parent envelope at m/z 361] by mass spectrometry and NMR spectroscopy. Anal. Found: C, 26.01; H, 10.13; B, 46.92; N, 15.28. Calcd for $C_8H_{36}B_{16}N_4$: C, 26.57; H, 10.04; B, 47.89; N, 15.50. Meanwhile the column was eluted further with ethyl acetate to isolate an additional fraction [R_F(anal.) = 0.6], which was evaporated and crystallized from hot benzene to give white needles [1.66 g; 27%]. These were identified as *exo*-6-(uro)-*arachno*-4-CB_8H_{12} (**4c**) by mass spectrometry and NMR spectroscopy [mp 174–175 °C; m/z(max) 252 ($[^{12}C_7{}^{14}N_4{}^{11}B_8{}^1H_{24}]^+$ requires 252) with the most intense peak, in the parent envelope at m/z 250]. Anal. Found: C, 32.63; H, 9.72; B, 33.91; N, 22.57. Calcd for $C_7H_{24}B_8N_4$: C, 33.51; H, 9.64; N, 22.34.

(b) From *exo*-6-(SMe_2)-*arachno*-4-CB_8H_{12} (4e). A solution of urotropine (500 mg; 3.57 mmol) and **4e** (180 mg; 1.04 mmol) in chloroform (15 mL) was heated at reflux for 4 h and then evaporated to dryness. The residual solids were extracted with dichloromethane (3 × 10 mL), silica gel (*ca.* 3 g) was added to the extracts, and the more volatile components were then evaporated off. The residual solid was placed onto a silica gel column (*ca.* 1.5 × 20 cm), and this was eluted with dichloromethane, followed by ethyl acetate (as described in the preceding experiment) successively to isolate compounds **4d** (50 mg; 26%) and **4c** (130 mg; 66%), identified as such by NMR spectroscopy.

***exo*-6-(SMe_2)-*arachno*-4-CB_8H_{12} (4d).** A sample of stock solution B [40 mL, containing 2.52 g (15 mmol) of $Na^+[nido\text{-}7,9\text{-}C_2B_{10}H_{13}]^-$,

(12) Kennedy, J. D.; Fontaine, X. L. R.; McGrath, M.; Spalding, T. R. *Magn. Reson. Chem.* **1991**, *29*, 711.
(13) McFarlane, W. *Proc. R. Soc. London, Ser. A* **1986**, *306*, 185.

prepared as described elsewhere,[8] was diluted with water (50 mL) and treated with succinic acid (2.36 g; 20 mmol) and dimethyl sulfide (10 mL), followed by stirring for 2 h. The mixture was then left standing 2 days and then shaken with benzene (40 mL). The aqueous and benzene layers were separated. The benzene layer was treated with water (50 mL) and the benzene removed by evaporation, leaving a pasty residue. This was extracted with chloroform (40 mL), and the upper (aqueous) layer was combined with that from the previous separation. The combined aqueous layers were then extracted with chloroform (20 mL), and the combined chloroform extracts were evaporated to dryness. This gave a white residue which was then washed with hexane (3 × 5 mL) and dried *in vacuo* to give white crystals [1.08 g (31%)], which were identified as *exo*-6-(SMe_2)-*arachno*-4-CB_8H_{12} (**4e**) by NMR spectroscopy. An analytical product [*m*/*z*(max) 174 ($[^{12}C_3{}^{11}B_8{}^1H_{18}{}^{32}S]^+$ requires *m*/*z* 174), with the most intense peaks in the parent envelope at *m*/*z* 166 and 173 and an intense fragmentation envelope around *m*/*z* 112 (corresponding to $[^{12}C^{11}B_8{}^1H_{12}]^+$)] was obtained by crystallization from dichloromethane/hexane as in the preceding experiment.

***exo*-6-(quin)-*arachno*-4-CB_8H_{12} (4f).** Quinoline (61 mg; 469 μmol) and compound **4e** (27 mg; 156 μmol) were heated at reflux in chloroform for 8 h. The mixture was then shaken with *ca.* 2% aqueous hydrochloric acid (10 mL), and the bottom layer was separated, dried over $MgSO_4$, filtered, and reduced in volume. Preparative TLC using chloroform as the liquid phase developed an orange band [R_F(prep) = 0.41], which was removed and extracted with dichloromethane to yield a yellow solid compound **4f** (32 mg; 85%). An analytical product, *m*/*z*(max) 241 ($[^{12}C_{10}{}^{14}N^{11}B_8{}^1H_{19}]^+$ requires *m*/*z* 241), identified as *exo*-6-(quin)-*arachno*-4-CB_8H_{12} by NMR spectroscopy, was obtained by crystallization from a benzene solution that was overlayered by the same volume of hexane.

***exo*-6-(MeCN)-*arachno*-4-CB_8H_{12} (4g).** A solution of compound **4e** (300 mg; 1.75 mmol) in acetonitrile (30 mL) was refluxed for 12 h. The mixture was then filtered, the acetonitrile evaporated, and the residual solid chromatographed on a silica gel column (*ca.* 2 × 30 cm). Elution with a mixture of dichloromethane and hexane (1:1, v/v) gave the main fraction of R_F(anal.) = 0.27, from which white crystals of **4g** (200 mg; 76%) were obtained by evaporation. An analytical product, *m*/*z*(max) 153 ($[^{12}C_3{}^{14}N^{11}B_8{}^1H_{15}]^+$ requires 153), identified as *exo*-6-(MeCN)-*arachno*-4-CB_8H_{12} by NMR spectroscopy, was obtained by crystallization from a dichloromethane solution that was overlayered by the same volume of hexane.

***exo*-6-(PPh_3)-*arachno*-4-CB_8H_{12} (4h).** A mixture of compound **4e** (300 mg; 1.75 mmol) and triphenylphosphine (500 mg; 1.91 mmol) was heated at reflux in toluene (30 mL) for 6 h. The toluene was evaporated and the residual solids separated by column chromatography on silica, using a mixture of dichloromethane and hexane (1:3, v/v) to isolate the main fraction of R_F(anal., 33% benzene in hexane) = 0.15. Further workup as in the preceding experiment gave a white solid compound **4h** (200 mg; 23%). An analytical product, *m*/*z*(max) 374 ($[^{12}C_{19}{}^{11}B_8{}^1H_{27}{}^{31}P]^+$ requires *m*/*z* 374), identified as *exo*-6-(PPh_3)-*arachno*-4-CB_8H_{12} by NMR spectroscopy, was obtained by crystallization from a dichloromethane solution that was overlayered by the same volume of hexane. Anal. Found: C, 60.19; H, 7.41; B, 22.87. Calcd for $C_{19}H_{27}B_8P$: C, 61.19; H, 7.30; B, 23.21.

***exo*-6-(MeNC)-*arachno*-4-CB_8H_{12} (4i).** To a solution of compound **4e** (500 mg; 2.91 mmol) in dichloromethane (25 mL) was added a solution of methyl isocyanide 0.5 mL) in dichloromethane (10 mL). The mixture was heated at reflux for 12 h and then filtered. Evaporation of the filtrate, followed by column chromatography of the residue on a silica gel column (*ca.* 2 × 30 cm) using a mixture of dichloromethane and hexane (1:1, v/v) as the liquid phase, gave the main fraction with of R_F(anal.) = 0.31. This was isolated and purified as in the preceding experiment to obtain *exo*-6-(MeNC)-*arachno*-4-CB_8H_{12} (**4i**), 200 mg (46%), *m*/*z*(max) 153, ($[^{12}C_3{}^{14}N^{11}B_8{}^1H_{15}]^+$ requires *m*/*z* 153), which was identified by NMR spectroscopy.

9-Me-8-(NMe_3)-*nido*-6-CB_9H_{10} (5a). Compound **3** (2.23 g; 11.4 mmol) was dissolved in acetone (30 mL), and this solution was treated with concentrated hydrochloric acid (0.1 mL) for 5 min at 10 °C. The solvents were then removed under reduced pressure (rotary evaporator) to leave a crystalline residue. This was dissolved in benzene (40 mL), and the solution was filtered. Silica gel (*ca.* 5 g) was added to the filtrate, the benzene was evaporated, and the solid residue was then transferred onto the top of a dry silica gel column (*ca.* 2.5 × 30 cm). Elution with benzene gave a minor fraction of **4a**, and subsequent elution with chloroform gave the main fraction [R_F(anal., $CHCl_3$) = 0.17], which was reduced in volume to *ca.* 20 mL, overlayered with hexane (*ca.* 40 mL), and left to crystallize for *ca.* 24 h. The resulting white needles of **5** were isolated by filtration and identified by NMR spectroscopy as 9-Me-8-(NMe_3)-*nido*-6-CB_9H_{10} (**5a**) as described below [yield 2.06 g (70%); mp 168–9 °C; *m*/*z*(max) 195 ($[^{12}Cs^{14}N^{11}B_9{}^1H_{22}]^+$ requires *m*/*z* 195)]. Anal. Found: C, 30.51; H, 11.53; B, 48.87; N, 7.31. Calcd for $C_5H_{22}B_9N$: C, 31.01; H, 11.45; B, 50.28; N, 7.23.

$[PPh_4]^+$[9-Me-8-(HO)-*nido*-6-$CB_9H_{10}]^-$·EtOH (5b). THF was evaporated from a sample of stock solution B [20 mL, containing 1.26 g (7.5 mmol) of Na^+[*nido*-7,9-$C_2B_{10}H_{13}]^-$, prepared as in ref 8] using a rotary evaporator. The remaining effervescent aqueous solution was immediately treated with acetone (20 mL) and left to stand overnight. The acetone was then evaporated and the remaining solution treated with 1 mol·L^{-3} tetramethylammonium chloride (*ca.* 2.5 mL) to remove the contaminant [*nido*-7,12-$C_2B_{10}H_{13}]^-$ anion.[8] The white precipitate was filtered off, and the filtrate was treated with a solution of $[PPh_4]Cl$ (1.9 g; 5 mmol) in water (*ca.* 30 mL), to obtain a white precipitate. This was filtered off and dissolved in hot 50% aqueous ethanol (ca. 30 mL); the warm mixture was refilterd, and the filtrate then left to crystallize for *ca.* 2 days to give lustrous prisms of **5b** (3.20 g; 80%), which were identified as $[PPh_4]^+$-[9-Me-8-(HO)-*nido*-6-$CB_9H_{10}]^-$·EtOH by NMR spectroscopy and X-ray diffraction analysis[14] as discussed below. Anal. Found: C, 60.94; H, 7.62; B, 17.96. Calcd for $C_{28}H_{40}B_9O_2P$: C, 62.42; H, 7.51; B, 18.13.

Single-Crystal X-ray diffraction Analysis of *exo*-6-(uro)-*arachno*-4-CB_8H_{12} (4c). Single crystals of **4c** were grown by slow crystallization from a dichloromethane solution that was overlayered by a twofold volume of hexane. All crystallographic measurements were carried out at 200 K on a Stoe STADI4 diffractometer using graphite-monochromated copper Kα X-radiation (λ = 154.184 pm). Data were collected in the range 4.0° < 2θ < 120.0° using ω/θ scans. No significant variation was observed in the intensities of three standard reflections. Lorentz and polarization corrections were applied to the data set together with semiempirical absorption based on azimuthal ψ-scans (maximum and minimum transmission factors 0.9261 and 1.00, respectively). The structure was solved by direct methods using SHELXS86[15] and was refined by full-matrix least squares using SHELX76.[16] All non-hydrogen atoms were refined with anisotropic thermal parameters. The methylene hydrogen atoms were constrained to predicted positions (CH = 96 pm) and were refined with an overall isotropic parameter. The cluster hydrogen atoms were located on a Fourier difference map and were freely refined with individual isotropic thermal parameters. The final Fourier difference map was essentially flat and contained no features of chemical significance (maximum and minimum residual electron density 0.17 and –0.29 e $Å^{-3}$, respectively). The weighting scheme used was $w = [\sigma(F_o) + 0.0004(F_o)^2]^{-1}$.

Crystal data for 4c: $C_7H_{24}B_8N_4$; 0.5 × 0.3 × 0.3 mm; *M* = 310.838; triclinic, space group $P\bar{1}$; *a* = 581.78(4), *b* = 1079.87(6), *c* = 1181.40(7) pm; α = 105.331(4), β = 92.312(4), γ = 92.797(4)°; *V* = 0.71127(8) nm^3; *Z* = 2; D_x = 1.45 Mg m^{-3}; μ = 0.562 mm^{-1}; *F*(000) = 328.

Data collection: Scan speeds 1.5–8.0° min^{-1}, ω scan widths 1.05° + α-doublet splitting, 4.0 < 2θ < 130.0°; 2339 data collected of which 2056 with $F_o > 4.0\sigma(F_o)$ considered observed.

Structure refinement: Number of parameters = 221, *R* = 0.0423, R_w = 0.0503, maximum Δ/σ = 0.002 [in *y*/*b* of H(**4a**)], mean Δ/σ = 0.000.

Results and Discussion

Syntheses. Dunks, Wiersema, and Hawthorne[9] reported some time ago that *closo*-1,2-$C_2B_{10}H_{12}$ (compound **1** in Scheme 1 and eq 1) can be converted into the [*nido*-7,9-$C_2B_{10}H_{13}]^-$ anion (compound **2** in Scheme 1 and eq 1. Recently we have reported[8]

$$\underset{\mathbf{1}}{1,2\text{-}C_2B_{10}H_{12}} \xrightarrow{2e^-} [C_2B_{10}H_{12}]^{2-} \xrightarrow[-OH^-]{H_2O} \underset{\mathbf{2}}{[C_2B_{10}H_{13}]^-} \quad (1)$$

a variation of this original method which affords a facile and convenient route to this species [see also path (i) in Scheme 1]. The anion **2** thus obtained can be conveniently used for further syntheses, including those now described in the following

(14) Šubrtová, V.; Petříček, V. *Acta Crystallogr.* **1990**, *C46*, 2419.
(15) Sheldrick, G. M. *SHELX 76, Program System for X-Ray Structure Determination*; University of Cambridge: Cambridge, U.K., 1976.
(16) Sheldrick, G. M. *J. Appl. Crystallogr.*, manuscript in preparation.

Scheme 1

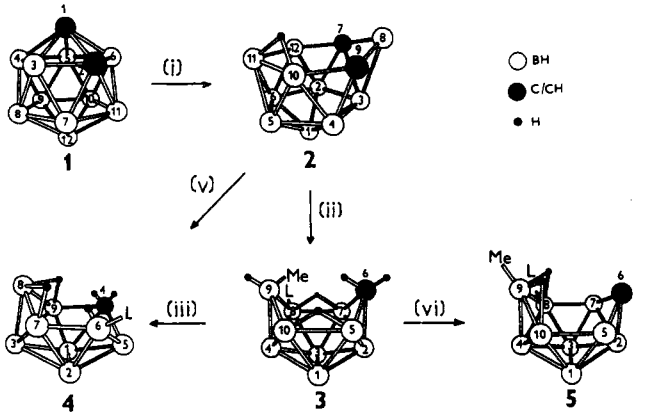

paragraphs, either in the form of its Na^+ salt solution in THF/H_2O (stock solution B of ref 8) or in the form of its $[NHMe_3]^+$ salt.[8]

Treatment of the $[NHMe_3]^+$ salt of anion **2** with aqueous trimethylamine in the presence of ethanol over a shorter reaction period (*ca.* 1 h) leads to the formation of ten-vertex *endo*-9-Me-8-(NMe_3)-*arachno*-6-CB_9H_{12} (compound **3** in Scheme 1) as the main isolated product [yield 76%; Scheme 1, path (ii); see also eq 2]. A small quantity of nine-vertex *exo*-6-(NMe_3)-

$$\underset{\mathbf{2}}{[C_2B_{10}H_{13}]^-} + H_3O^+ + 2H_2O + NMe_3 \rightarrow \underset{\mathbf{3}}{CH_3(NMe_3)CB_9H_{12}} + B(OH)_3 + H_2 \quad (2)$$

$$\underset{\mathbf{3}}{CH_3(NMe_3)CB_9H_{12}} + 2H_2O \rightarrow CH_3B(OH)_2 + \underset{\mathbf{4a}}{NMe_3CB_8H_{12}} + H_2 \quad (3)$$

$$\underset{\mathbf{2}}{[C_2B_{10}H_{13}]^-} + H_3O^+ + 4H_2O + L \rightarrow \underset{\mathbf{4}}{LCB_8H_{12}} + CH_3B(OH)_2 + B(OH)_3 + 2H_2 \quad (4)$$

arachno-4-CB_8H_{12} [compound **4**, L = NMe_3 (**4a**), in Scheme 1] is also formed. This last compound **4a** is the only product, obtainable in a high yield (91%), when ethanol is replaced by chloroform and the reaction time is extended to *ca.* 3 h [path (v) in Scheme 1 and eq 4]. Compound **4a** is also readily formed in the reaction between the ten-vertex compound **3** and aqueous trimethylamine in the presence of ethanol and chloroform [path (iii) in Scheme 1 and eq 3], thus reasonably confirming that **3** is an intermediate along the degradation pathway from anion **2** to give **4a**, with the stepwise stoichiometry being as in eqs 2–4, respectively.

Using anion **2** as its Na^+ salt in THF/H_2O (stock solution B of ref 8) and an excess of the appropriate base L, we have also been able to isolate a series of additional *arachno* nine-vertex compounds *exo*-6-L-*arachno*-4-CB_8H_{12}, where L = py (compound **4b**), urotropine (uro) (compound **4c**), and SMe_2 (compound **4e**), in each case as the sole neutral carborane products, in yields of 23–63% [path (v) in Scheme 1; stoichiometry as in eq 4]. In the urotropine reaction, the interesting bis(carborane) species *exo,exo'*-6,6'-uro-(*arachno*-4-CB_8H_{12})$_2$ (**4d**) was isolated as an additional product, in 27% yield. For all these reactions the reaction time was longer (2–4 days), and in the cases of L = SMe_2 and uro, the reactions were carried out in the presence of succinic acid in order to enhance the degradation.

We expected that the SMe_2 ligand in compound **4e** might be susceptible to displacement by stronger Lewis bases, and this proved to be so. Thus, Lewis bases L, where L = py, quin, uro,

Scheme 2

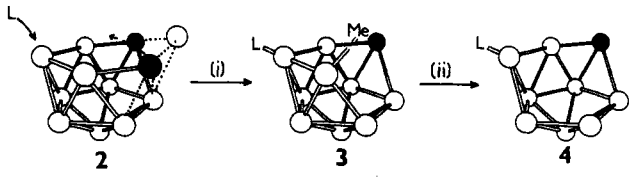

MeCN, PPh_3, and MeNC, react smoothly with compound **4e** in refluxing chloroform or toluene solutions to generate the corresponding compounds *exo*-6-L-*arachno*-4-CB_8H_{12} (**4b,f–i**, respectively). Isolatable yields are variable to good (23–88%), and again in the urotropine reaction the bis(carborane) base adduct **4d** is formed (26% yield).

The structures as represented in Scheme 1 suggest mechanistic insight into the degradation reactions of the [*nido*-7,9-$C_2B_{10}H_{13}$]$^-$ anion **2** presented above, which are, uniquely, characterized by the loss of one {CH} vertex from the cluster. Thus it is reasonable to suggest hydrolytic elimination of the {BH(8)} vertex in **2** (for which there is precedent; compare ref 8), together with an attack by base at the B(11) site and a concomitant extrusion of the {CH(9)} unit from the cluster to form the methyl group in an *endo* position on B(10) (numbering as in **2**), thus leading to compound **3** [path (i) in Scheme 2].

Further hydrolytic attack at, and elimination of, the formed or incipient {BH(9)Me} vertex in **3** then leads directly to the nine-vertex *arachno* compounds **4** [path (ii) in Scheme 2]. This proposed reaction pathway is supported experimentally by the rapid degradation of **3** into **4a** when ethanol and aqueous trimethylamine are used as degradation agents at room temperature.

Of interest in this area, and also potentially significant for further synthetic work, is our observation of a direct *arachno* to *nido* conversion in the reaction between the intermediate compound **3** and acetone [path (vi) in Scheme 1; see also eq 5].

$$\underset{\mathbf{3}}{Me(NMe_3)CB_9H_{12}} + Me_2CO \rightarrow Me_2CHOH + \underset{\mathbf{5a}}{Me(NMe_3)CB_9H_{10}} \quad (5)$$

In the presence of concentrated hydrochloric acid this yields the *nido* ten-vertex compound 9-Me-8-(NMe_3)-6-CB_9H_{10} (**5a**) (structure **5** for L = NMe_3 in Scheme 1), isolatable as the only neutral cluster product in 70% yield. The reaction is consistent with the redox stoichiometry outlined in eq 5. Of the same constitution is the [9-Me-8-(HO)-*nido*-6-CB_9H_{10}]$^-$ anion **5b** (structure **5** in Scheme 1, L = OH^-), which can be prepared from anion **2** (aqueous THF solution of the sodium salt, stock solution B)[8] by evaporation of THF and treatment of the remaining aqueous solution with acetone. The overall stoichiometry as in eq 6is

$$\underset{\mathbf{2}}{[C_2B_{10}H_{13}]^-} + 4H_2O + Me_2CO \rightarrow \underset{\mathbf{5b}}{[CH_3(HO)CB_9H_{10}]^-} + B(OH)_3 + Me_2CHOH + H_2 \quad (6)$$

consistent with the net loss of the B(8) boron vertex from the cage of **2**, resulting in the formation of an unstable [9-Me-8-(HO)-*arachno*-6-CB_9H_{12}]$^-$ intermediate anion [see path (i) in Scheme 2 and also structure **3** in Scheme 1, L = OH^-], which is then oxidized by acetone to give the *nido* compound **5b**.

Anion **5b** was precipitated from the reaction mixture as its $[PPh_4]^+$ salt after removing the acetone and quenching the contaminant [7,12-$C_2B_{10}H_{13}$]$^-$anion[8] by tetramethylammonium chloride and then adding $[PPh_4]Cl$ to the resulting solution. The salt of **5b** anion thus obtained was recrystallized from hot 50% aqueous ethanol and thereby isolated as the ethanol solvate $[PPh_4]^+$[9-Me-8-(HO)-*nido*-6-CB_9H_{10}]$^-$·EtOH. The structure

Table 1. Assigned ^{11}B NMR Parameters for Ten-Vertex *Arachno* and *Nido* Compounds of Type **3**, **5**, and **8**

	compound			
assgnt[a]	**3**[b]	**5a**[b]	**5b**[c]	**8**[d,e]
B(1)	−39.6 (145)	−5.9 (147[f])	−4.0 (131)	} +4.5 (133)[g]
B(3)	−34.1 (140)	−5.9 (147[f])	−7.7 (132)	
B(2)	−11.6 (159)	−32.5 (155[f])	−36.3 (144[f])	−30.6 (143)
B(4)	+5.6 (142)	−32.5 (155[f])	−36.3 (144[f])	−37.6 (143)
B(5)	−8.5 (150[f])	+5.6 (142)	−3.2 (135[f])	} +1.9 (135)[g]
B(7)	−8.1 (153)	+0.5 (137)	+5.9 (143)	
B(8)	−14.5[h]	−4.8[h]	+7.6[h]	} −12.3 (140)[g]
B(10)	−24.5 (144)	−14.3 (156)	−26.5 (134/35[i])	
B(9)	+5.6 (110)	**8.0**[h]	−0.9 (29[i])	−1.7 (175)

[a] Assignment by [^{11}B–^{11}B]-COSY and [^1H–^1H]-COSY (for **3** and **5a**) experiments; chemical shifts $\delta(^{11}B)$ at 294–297 K, coupling constants $^1J(^{11}B–^1H)$ in parentheses. [b] In CD_2Cl_2. [c] In CD_3CN. [d] In $CDCl_3$. [e] $[PPh_4]^+$ salt. [f] Approximate value (peak overlap). [g] Signals of relative intensity 2; other signals are of relative intensity 1. [h] Singlet for the substituted atom; other signals are doublets. [i] Coupling constant $^1J(^{11}B–\mu\text{-}^1H)$.

Table 2. Assigned ^1H NMR Parameters for Ten-Vertex *Arachno* and *Nido* Compounds of Type **3**, **5**, and **8**

	compound			
assgnt[a]	**3**[b]	**5a**[b]	**5b**[c]	**8**[d,e]
H(1)	+0.36	+2.31	+2.26	} +2.39[f]
H(3)	+0.62	+2.47	+2.26	
H(2)	+2.17	−0.03	−0.42	+0.07
H(4)	+3.51	+1.07	+0.62	+0.34
H(5)	+2.48	+3.41	+2.80	} +3.22[f]
H(7)	+2.86	+3.31	+3.22	
H(6)	+0.35/−0.24[g]	+5.74[h]	+5.19[i]	+5.56[j]
H(8)	+2.89[k]	+3.08[k]	+3.12[k]	} +1.89[f]
H(10)	+1.04	+1.84	+1.02	
H(9)	+2.78[l]	+0.76[m]	+0.29[m]	+2.79
μ-H_1	−1.56[n]	−0.63[o]	−0.68[o]	} −3.61[f]
μ-H_2	−3.81[p]	−3.01[q]	−3.05[q]	

[a] Assignment by ^1H–{^{11}B(selective)} and [^1H–^1H]-COSY (for **3** and **5a**) experiments; chemical shifts $\delta(^1H)$ at 294–297 K. [b] In CD_2Cl_2. [c] In CD_3CN. [d] In $CDCl_3$. [e] $[PPh_4]^+$ salt. [f] Signals of *exo* and *endo* hydrogens, respectively. [h] Fine doublet splitting *ca.* 4 Hz observed in ^1H–{^{11}B(broad band noise)} experiment. [i] Fine quartet splitting observed in ^1H–{^{11}B(broad band noise)} experiment. [j] Fine structure, splitting *ca.* 6 Hz, observed in ^1H–{^{11}B(broad band noise)} experiment. [k] Signals of the NMe_3 methyls. [l] Signal of the *exo* hydrogen; additional signal of the *endo* B(9)Me methyl at +0.35 ppm. [m] Signals of the Me substituent. [n] μ-H(7,8). [o] μ-H(8,9). [p] μ-H(5,10). [q] μ-H(9,10).

of this compound has been determined by an X-ray diffraction study[14] that fully confirmed the cluster constitution **5** and additionally revealed an interesting solid-state bonding mode in which two [9-Me-8-HO-*nido*-6-CB_9H_{10}]$^-$ molecules are joined together *via* hydrogen-bridge bonding involving two molecules of ethanol and the two 8-(OH) substituents.

NMR Spectroscopy. All compounds were identified by NMR spectroscopy allied with mass spectrometry to confirm the molecular formulas. ^{11}B and ^1H NMR spectroscopy, making use of [^{11}B–^{11}B]-COSY, [^1H–^1H]-COSY (see also Figure 5) and ^1H{^{11}B(selective)} techniques, resulted in the assignment of all the ^{11}B and ^1H resonances to their individual cluster positions for all compounds of the type **3**–**5**. A comparison of cluster shielding patterns with those of the structurally related unsubstituted parent carborane analogs is therefore possible.

Measured NMR data for the ten-vertex *arachno* monocarbaborane *endo*-9-Me-8-(NMe_3)-*arachno*-6-CB_9H_{12} (**3**) are in Tables 1 and 2, and proton and ^{11}B chemical shifts, together with those of the unsubstituted "parent" [*arachno*-6-CB_9H_{14}]$^-$ anion (compound **6**)[17,18] for comparison, are present graphically in

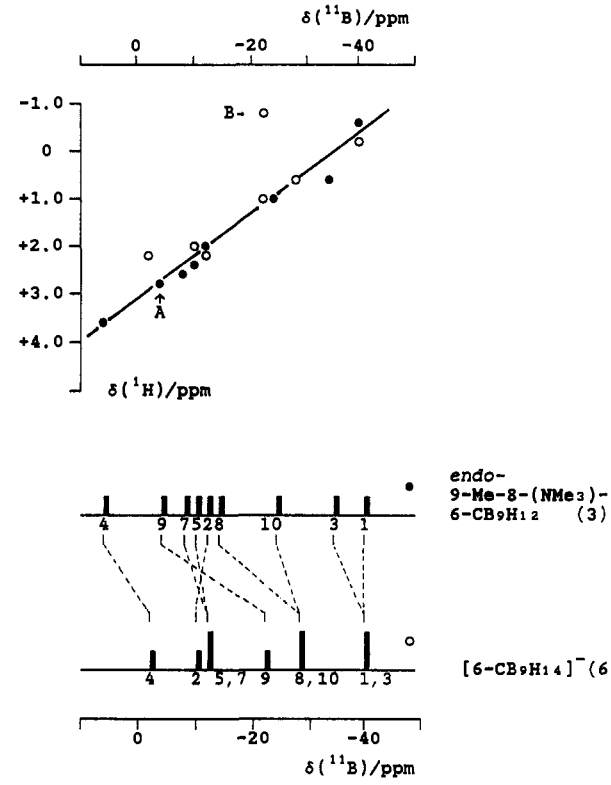

Figure 1. Plot of $\delta(^1H)$ *versus* $\delta(^{11}B)$ for the *arachno* monocarbaboranes *endo*-9-Me-8-(NMe_3)-6-CB_9H_{12} (**3**, ●) and [6-CB_9H_{14}]$^-$ (**6**, ○) (data from refs 17 and 18). The line has slope $\delta(^1H)/\delta(^{11}B)$ *ca.* 1:13 and intercept +2.9 ppm in $\delta(^1H)$. Point A is the datum for the *exo*-BH(9) unit in compound **3**, and point B relates to that of the *endo*-BH(9) unit in compound **6**. Bottom: Comparison of the ^{11}B chemical shifts and relative intensities for both compounds.

Figure 1. The NMR data for **3** are seen to be entirely consistent with the proposed ten-vertex *arachno* constitution of the compound, and in particular it is apparent that there are close shielding parallels with the parent unsubstituted [*arachno*-6-CB_9H_{14}]$^-$ model species **6**. As can be seen from the bottom part of Figure 1, the most significant differences in ^{11}B shieldings between **3** and **6** arise from the α-substituent effects in **3** of the 8-(NMe_3) and *endo*-Me substituents, which induce substantial shifts to low field of *ca.* 14 and 19 ppm respectively compared to unsubstituted **6**. These are within expected ranges. Compared to these, the (additive) β and γ effects are relatively minor, with the basic shielding pattern and the shielding sequence remaining essentially unchanged, although it should be noted that there is an overall decrease in mean cluster ^{11}B shielding [from $\delta(^{11}B)$ *ca.* −22 to *ca.* −15.5 ppm] from anionic **6** to neutral **3**.

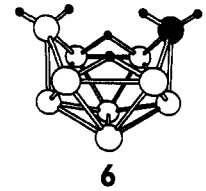

6

Some interest in **3** derives from the identification of the BH(9) terminal proton as *exo* and the positioning of the 9-methyl substituent thereby as *endo*. There are two pieces of evidence for this. First, the (^{11}B, ^1H) datum (point A in Figure 1) for BH(9) falls close to the ^{11}B:^1H(exo) correlation line whereas data for *endo* or bridging hydrogen sites generally lie well above this plot [see the BH(9) datum for compound **6**, point B in Figure 1, for example]. This behavior has been observed in other *endo*-

(17) Štíbr, B.; Jelínek, T.; Plešek, J.; Heřmánek, S. *J. Chem. Soc., Chem. Commun.* **1987**, 963.
(18) Fontaine, X. L. R.; Kennedy, J. D.; Thornton-Pett, M.; Nestor, K.; Štíbr, B.; Jelínek, T.; Baše, K. *J. Chem. Soc., Dalton Trans.* **1990**, 2887.

Table 3. Assigned ^{11}B NMR Parameters for the Nine-Vertex 6-L-*arachno*-4-CB_8H_{12} Compounds (4)

	compound								
assgnt[a]	4a[b]	4b[c]	4c[b]	4d[b]	4e[c]	4f[c]	4g[c]	4h[c]	4i[c]
B(1)	−21.9 (157)	−20.8 (157)	−21.6 (158)	−21.1 (159)	−19.9 (159)	−20.5 (155)	20.2 (159)	−19.1 (152)	−19.0 (159)
B(2)	−11.9 (135)	−8.7 (137)	−13.3 (136)	−12.6 (137)	−9.0 (141)	−7.7 (136)	−8.8 (142)	−10.6 (135)	−10.2 (143)
B(3)	−52.6 (145)	−52.6 (146)	−52.9 (147)	−53.1 (147)	−51.1 (148)	−51.6 (147)	−52.3 (148)	−51.2 (145)	−51.8 (136[d])
B(5)	+0.2 (147[d])	+1.2 (145[d])	−1.0 (145)	−1.9 (145)	+0.1 (146[d])	+1.7 (142[d])	−0.5 (160[d])	−2.0 (*e*)	+1.7 (141)
B(6)	−18.7 (122)	−22.8 (128[d])	−24.6 (134[d])	−23.8 (142[d])	−31.5 (130)	−25.1 (138[d])	−36.1 (124)	−44.4 (*e*)	−52.4 (120[d])
B(7)	−4.6 (140)	−2.8 (139[d])	−5.8 (138)	−5.6 (140)	−4.5 (140)	−2.8 (135[d])	−2.8 (145)	−2.6 (128)	−2.3 (147)
B(8)	−24.9 (150)	−24.0 (179[d])	−24.6 (134[d])	−23.8 (142[d])	−22.8 (153/36[f])	−23.7 (170[d])	−23.2 (154[g])	−22.8 (134)	−22.5 (155[g])
B(9)	−0.3 (147[d])	+0.1 (153[d])	+0.2 (152)	+0.7 (150)	+1.2 (145[d])	+0.7 (133[d])	+1.8 (154)	+3.1 (147)	+3.4 (155)

[a] Assignment by [^{11}B–^{11}B]-COSY (for **4a,b,d,f,e**) and [^1H–^1H]-COSY (for **4a**) experiments; chemicals shifts $\delta(^{11}B)$ at 274–276 K, coupling constants $^1J(^{11}B$–$^1H)$ in parentheses. [b] In CD_2Cl_2. [c] In $CDCl_3$. [d] Approximate value (peak overlap). [e] Broad signal. [f] Coupling constant $^1J(^{11}B$–μ-$^1H)$. [g] Apparent signal broadening due to coupling to μ-H.

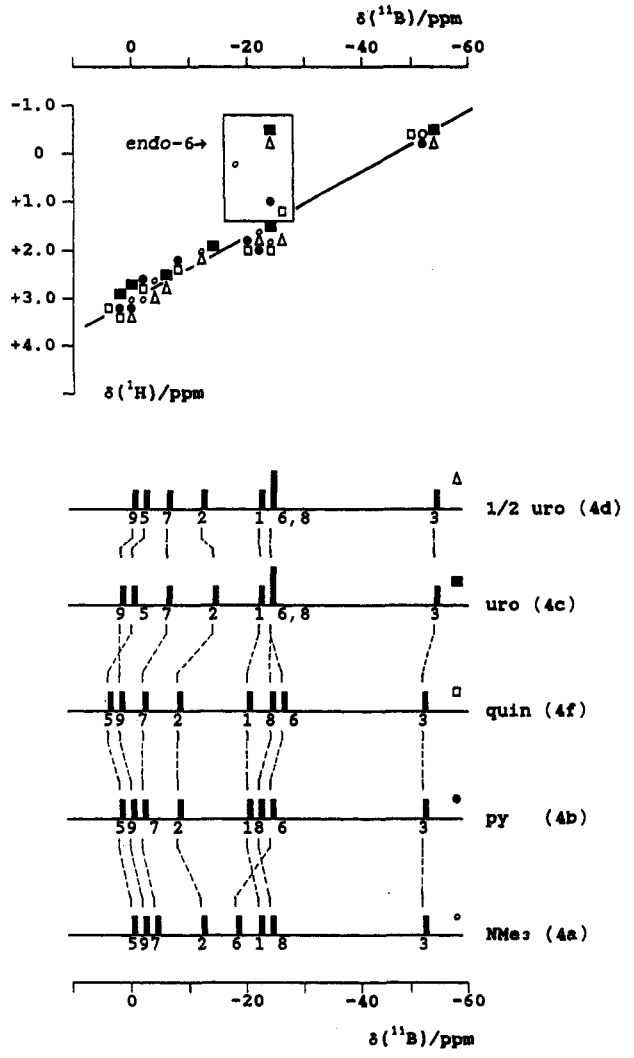

Figure 2. Top: Plot of $\delta(^1H)$ *versus* $\delta(^{11}B)$ for the *arachno* monocarbaboranes *exo*-6-L-4-CB_8H_{12} [when L = NMe_3 (**4a**, ○) py (**4b**, ●), quin (**4f**, □), and uro (**4c**, ■)] and *exo,exo'*-6,6'-(uro)-(4-$CB_8H_{12})_2$ (**4d**, △). The line drawn has slope $\delta(^1H)/\delta(^{11}B)$ *ca.* 1:15 and intercept +3.1 in $\delta(H^1)$. Bottom: Comparison of the ^{11}B chemical shifts and relative intensities for all compounds.

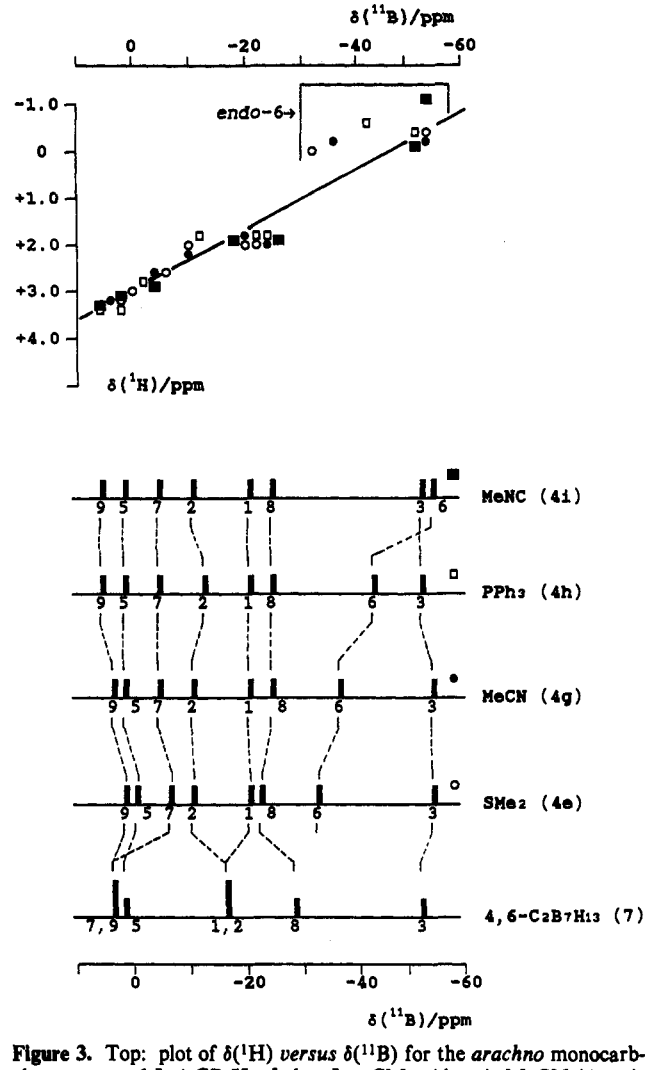

Figure 3. Top: plot of $\delta(^1H)$ *versus* $\delta(^{11}B)$ for the *arachno* monocarbaboranes *exo*-6-L-4-CB_8H_{12} [when L = SMe_2 (**4e**, ○), MeCN (**4g**, ●), PPh_3 (**4h**, □), and MeNC (**4i**, ■)]. The line drawn has slope $\delta(^1H)/\delta(^{11}B)$ *ca.* 1:15 and intercept +2.8 in $\delta(^1H)$. Bottom: Comparison of the ^{11}B chemical shifts and relative intensities for both compounds with those of the dicarbaborane analogue *arachno*-4,6-$C_2B_7H_{13}$ (**7**) (data from ref 22).

substituted *arachno* ten-vertex systems such as $[SB_9H_{13}OH]^-$ [19] and $[B_{10}H_{13}CN]^{2-}$.[20] Second, in [^1H–^1H]-COSY experiments, no interproton correlation was observed between this proton and either of the $^1H(\mu$-7,8) or $^1H(\mu$-5,10) sites (Figure 5, lower part), whereas the $^1H(6)$ *endo* position does exhibit coupling to these bridging positions, as does the equivalent $^1H(6)$(*endo*) position to the $^1H(\mu$-7,8) bridge in the nine-vertex compound **4a** (see Figure 5). This also suggests that $^1H(9)$ has non-*endo* and therefore *exo* character, consistent with the proposed *endo*-9-Me substituent configuration.

The measured NMR data for the new nine-vertex *arachno* monocarbaboranes *exo*-6-L-*arachno*-4-CB_8H_{12} (compounds **4a–i**) are in Tables 3 and 4. Aspects of the ^{11}B and ^1H shielding behavior are presented graphically in Figures 2 and 3, the latter also containing data for the isostructural unsubstituted dicarb-

(19) Bown, M.; Fontaine, X. L. R.; Kennedy, J. D. *J. Chem. Soc., Dalton Trans.* **1988**, 1467.
(20) Baše, K.; Alcock, N. W.; Howarth, O. W.; Powell, H. R.; Harrison, A. T.; Wallbridge, M. G. H. *J. Chem. Soc., Chem. Commun.* **1988**, 348.

Table 4. Assigned ^1H NMR Parameters for Nine-Vertex 6-L-*arachno*-4-CB_8H_{12} Compounds (4)

	compound								
assgnt[a]	**4a**[b]	**4b**[c]	**4c**[b]	**4d**[b]	**4e**[c]	**4f**[c]	**4g**[c]	**4h**[c]	**4i**[c]
H(1)	+1.70	+1.86	+1.75	+1.81	+1.91	+2.01	+1.92	+1.98	+2.00
H(2)	+2.09	+2.16	+1.89	+1.97	+2.10	+2.40	+2.15	+1.84	+2.05
H(3)	−0.49	−0.32	−0.49	−0.45	−0.37	−0.21	−0.34	−0.32	−0.30
H(4)(*exo*)	−0.10	+0.07	−0.12	0.00	+0.02[d]		+0.02	+0.15	+0.07
H(4)(*endo*)	−1.24	−1.14	−1.23	−1.20	−1.10[e]	−0.91	−1.29	−0.50	−0.86
H(5)	+2.96	+3.14	+2.97	+2.97	+3.04	+3.24	+3.07	+3.21	+3.11
H(6)[f]	+0.21	+1.09	−0.51	−0.32	−0.08	+1.22	+0.12	−0.53	−1.13
H(7)	+2.52	+2.68	+2.55	+2.62	+2.58	+2.74	+2.69	+2.67	+2.73
H(8)	+1.76	+1.95	+1.79	+1.89	+2.00	+2.00	+1.99	+2.09	+2.07
H(9)	+2.98	+3.12	+3.01	+3.06	+3.11	+3.26	+3.14	+3.26	+3.25
μ-H(7,8)	−2.85	−2.58	−2.95	−2.93	−2.85	−2.42	−2.81	−2.36	−2.92
μ-H(8,9)	−2.21	−2.00	−2.23	−2.20	−2.01	−1.83	−2.07	−1.79	−1.95

[a] Assignment by ^1H–{^{11}B(selective)}, [^{11}B–^{11}B]-COSY (for **4a,b,d,f,e**), and [^1H–^1H]-COSY (for **3** and **5a**) experiments; chemical shifts $\delta(^1H)$ at 294–297 K. [b] In CD_2Cl_2. [c] In $CDCl_3$. [d] Quartet on ^1H–{^{11}B(broad band)} decoupling, repeated splitting ca. 5.5 Hz. [e] Quartet on ^1H–{^{11}B(broad band)} decoupling, repeated splitting ca. 9.5 Hz. [f] Signals of the exoskeletal ligand: **4a**, +2.80 (9H, NMe_3); **4b**, +8.80 to +7.56 (5H, py); **4c**, +4.68 to +4.40 (12H, uro); **4d**, +4.75 to +4.40 (12H, uro); **4e**, +2.74, +2.44 (3 + 3H, SMe_2); **4f**, +9.30 to +7.60 (9H, quin); **4g**, +2.45 (3H, MeCN); **4h**, +7.60 to +7.2 (15H, PPh_3); **4i**, +3.55 (3H, MeNC).

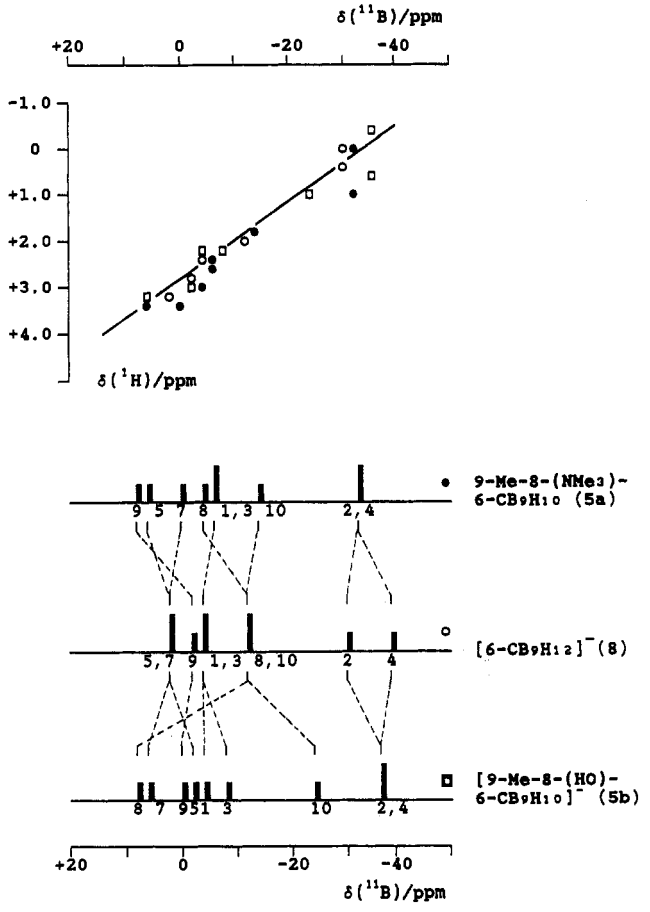

Figure 4. Top: Plot of $\delta(^1H)$ *versus* $\delta(^{11}B)$ for the *nido* monocarbaboranes 9-Me-8-(NMe_3)-6-CB_9H_{10} (**5a**, ●), [9-Me-8-HO-*nido*-6-CB_9H_{10}]$^-$ (**5b**, □), and [6-CB_9H_{12}]$^-$ (**8**, ○). The line drawn has slope $\delta(^1H)/\delta(^{11}B)$ *ca.* 1:13 and intercept +2.8 in $\delta(^1H)$. Bottom: Comparison of the ^{11}B chemical shifts and relative intensities for both compounds.

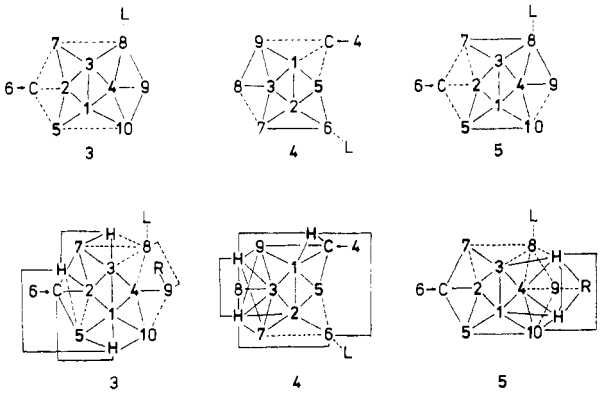

Figure 5. Typical [^{11}B–^{11}B]-COSY (upper part) and [^1H–^1H]-COSY NMR (bottom part) correlations for compounds of type **3a**, **4b**, and **5c**. Unobserved cross-peaks are indicated by hatched lines.

aborane congener *arachno*-4,6-$C_2B_7H_{13}$ (structure **7**).[21,22] The NMR data for compounds **4a–f**, together with the mass spectrometric results, are in excellent agreement with the proposed constitution (structure **4** in Scheme 1). Intercomparison of the ^{11}B shielding patterns (lower part of Figures 2 and 3) reveals very similar shielding behavior, the main differences arising from the changes in the ligand-substituent effect at the 6-position, with trivial differences in ordering among other closely spaced signals arising from longer-range effects. There is also a striking similarity in shielding with that of the isostructural dicarbaborane congener *arachno*-4,6-$C_2B_7H_{13}$ (**7**) (see lowest trace in Figure 3), from which the general structure **4** can be notionally derived by the isolobal[23,24] replacement of one {CH_2} unit at the (6) position. The individual [$\delta(^{11}B)$, $\delta(^1H)$] data points for all the compounds of type **4** (Figures 2 and **3**, upper diagrams) all fall close to a single $\delta(^{11}B)$:$\delta(^1H)$ correlation line, except for the more highly shielded $^1H(6)$(*endo*) position as already mentioned above.

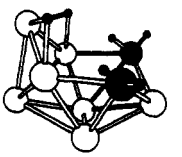

7

Measured NMR data for the ten-vertex *nido* monocarbaboranes of type **5**, 9-Me-8-L-*nido*-6-CB_9H_{10} (L = NMe_3 and OH^-; **5a,b**, respectively), are in Tables 1 and 2, and proton and ^{11}B chemical shifts, together with those of the unsubstituted parent [*nido*-6-CB_9H_{12}]$^-$anion (compound **8**)[21,22] are shown graphically in Figure 4. The NMR data for both compounds **5a,b** are clearly in good agreement with the proposed structures (see **5** in Scheme 1). The most striking differences between **5** and unsubstitured

(21) Dolanský, J.; Heřmánek, S.; Zahradník, R. *Collect. Czech. Chem. Commun.* **1981**, *46*, 2479.
(22) Jelínek, T.; Heřmánek, S.; Štíbr, B.; Plešek, J. *Polyhedron* **1986**, *5*, 1303.
(23) Elian, M.; Hoffman, R. *Inorg. Chem.* **1975**, *14*, 1058.
(24) Hoffman, R. *Science* (Washington, D.C.) **1981**, *211*, 995.

Table 5. Non-Hydrogen Atom Coordinates ($\times 10^4$) and Their Equivalent Isotropic Thermal Parameters ($Å^2 \times 10^3$) Together with Cluster Hydrogen Atom Coordinates ($\times 10^3$) and Their Isotropic Thermal Parameters for **4c** with Estimated Standard Deviations (Esd's) in Parentheses

atom	*x*	*y*	*z*	$U_{eq}{}^a/U_{iso}$
N(1)	1929(2)	3778(1)	7301(1)	20.4(4)
N(2)	2289(2)	1811(1)	7966(1)	31.8(4)
N(3)	1677(2)	1644(1)	5869(1)	28.1(4)
N(4)	−1427(2)	2246(1)	7115(1)	31.2(5)
C(12)	3071(3)	3151(1)	8204(1)	29.2(5)
C(13)	2469(3)	2986(1)	6090(1)	27.2(5)
C(14)	−655(2)	3593(1)	7339(1)	27.9(5)
C(23)	2822(3)	1122(1)	6778(1)	31.2(5)
C(24)	−230(3)	1706(1)	7999(1)	35.0(6)
C(34)	−838(3)	1544(1)	5943(1)	31.4(6)
B(1)	1964(4)	7814(2)	8706(2)	39.0(7)
B(2)	996(3)	6398(2)	7654(2)	29.1(6)
B(3)	2002(3)	7761(2)	7189(2)	28.9(6)
C(4)	4610(4)	7602(2)	9257(2)	48.1(7)
B(5)	2537(4)	6347(2)	8964(2)	37.7(6)
B(6)	3002(3)	5227(1)	7590(1)	22.7(5)
B(7)	2676(3)	6146(2)	6453(1)	27.1(5)
B(8)	4647(3)	7580(2)	6687(2)	30.7(6)
B(9)	4500(3)	8452(2)	8213(2)	34.7(6)
H(1)	99(3)	852(2)	931(2)	49(5)
H(2)	−77(3)	602(2)	740(2)	45(5)
H(3)	74(3)	831(2)	680(2)	39(5)
H(4a)	593(4)	707(2)	895(2)	58(6)
H(4b)	492(4)	811(2)	1005(2)	62(6)
H(5)	165(3)	605(2)	966(2)	47(5)
H(6)	487(3)	521(1)	765(1)	25(4)
H(7)	198(3)	571(2)	553(2)	41(5)
H(8)	504(3)	805(2)	599(2)	51(5)
H(9)	496(4)	949(2)	843(2)	54(6)
H(78)	493(3)	646(2)	650(2)	50(5)
H(89)	606(3)	785(2)	749(2)	49(5)

^{a} U_{eq} = $^1/_3$ × trace of the orthogonalized U_{ij} matrix.

Table 6. Interatomic Distances (pm) for **4c** with Esd's in Parentheses

C(12)–N(1)	153.1(4)	C(13)–N(1)	152.7(4)
C(14)–N(1)	151.3(4)	B(6)–N(1)	159.4(4)
C(12)–N(2)	144.1(3)	C(23)–N(2)	147.1(3)
C(24)–N(2)	146.9(3)	C(13)–N(3)	144.7(3)
C(23)–N(3)	146.6(3)	C(34)–N(3)	146.8(3)
C(14)–N(4)	144.9(3)	C(24)–N(4)	146.8(3)
C(34)–N(4)	147.1(3)		
B(2)–B(1)	173.0(5)	B(3)–B(2)	179.1(4)
B(3)–B(1)	178.0(4)		
C(4)–B(1)	167.1(5)	B(8)–B(3)	169.7(4)
B(5)–B(1)	173.4(4)	B(7)–B(3)	180.9(4)
B(9)–B(1)	180.2(5)	B(9)–B(3)	180.3(4)
B(5)–B(2)	173.8(4)	B(7)–B(2)	175.9(4)
B(6)–B(2)	175.3(4)		
B(5)–C(4)	171.3(5)	B(8)–B(7)	182.7(4)
B(9)–C(4)	172.0(4)	B(9)–B(8)	181.1(5)
B(6)–B(5)	180.0(4)	B(7)–B(6)	187.1(4)
H(1)–B(1)	111(2)	H(3)–B(3)	111(2)
H(2)–B(2)	108(2)		
H(4a)–C(4)	102(2)	H(4b)–C(4)	95(2)
H(5)–B(5)	111(2)	H(7)–B(7)	110(2)
H(6)–B(6)	109(2)	H(9)–B(9)	109(2)
H(8)–B(8)	111(2)		
H(78)–B(7)	133(2)	H(89)–B(9)	137(2)
H(78)–B(8)	120(2)	H(89)–B(8)	116(2)

8 again arise from the α-substituent effects of the 8-(NMe_3), OH^-, and the 9-Me substituents, although the shifts to lower field, of *ca.* 8 and 10 (for **5a**) ppm, respectively are both smaller than those between the *arachno* congeners **3** and **6** discussed above. The overall decrease in mean cluster ^{11}B shielding [from $\delta(^{11}B)$ *ca.* −11 to *ca.* −9 ppm] is also much smaller than for the corresponding *arachno* pair. It should be noted that the ^1H shielding parameters and the [^{11}B–^{11}B]-COSY correlations for anion **8** (Figure 5) are previously unreported. The COSY correlations now confirm the previous[25] ^{11}B assignments.

Table 7. Selected Angles (deg) between Interatomic Vectors for **4c** with Esd's in Parentheses

B(3)–B(1)–B(2)	61.3(2)	C(4)–B(1)–B(2)	106.8(2)
C(4)–B(1)–B(3)	109.3(2)	B(5)–B(1)–B(2)	60.2(2)
B(5)–B(1)–B(3)	111.7(2)	B(5)–B(1)–C(4)	60.4(2)
B(9)–B(1)–B(2)	107.0(2)	B(9)–B(1)–B(3)	60.4(2)
B(9)–B(1)–C(4)	59.2(2)	B(9)–B(1)–B(5)	108.6(2)
B(3)–B(2)–B(1)	60.7(2)	B(5)–B(2)–B(1)	60.0(2)
B(5)–B(2)–B(3)	111.0(2)	B(6)–B(2)–B(1)	111.2(2)
B(6)–B(2)–B(3)	114.1(2)	B(6)–B(2)–B(5)	62.1(2)
B(7)–B(2)–B(1)	110.5(2)	B(7)–B(2)–B(3)	61.3(2)
B(7)–B(2)–B(5)	113.5(2)	B(7)–B(2)–B(6)	64.4(2)
B(2)–B(3)–B(1)	58.0(2)	B(7)–B(3)–B(1)	106.1(2)
B(7)–B(3)–B(2)	58.5(2)	B(8)–B(3)–B(1)	114.4(2)
B(8)–B(3)–B(2)]	112.0(2)	B(8)–B(3)–B(7)	62.7(2)
B(9)–B(3)–B(1)	60.4(2)	B(9)–B(3)–B(2)	104.4(2)
B(9)–B(3)–B(7)	105.6(2)	B(9)–B(3)–B(8)	62.2(2)
B(5)–C(4)–B(1)	61.6(2)	B(9)–C(4)–B(1)	64.2(2)
B(9)–C(4)–B(5)	113.5(2)	H(4a)–C(4)–B(1)	135.5(12)
H(4a)–C(4)–B(5)	96.7(13)	H(4a)–C(4)–B(9)	96.1(13)
H(4b)–C(4)–B(1)	110.4(14)	H(4b)–C(4)–B(5)	117.4(14)
H(4b)–C(4)–B(9)	115.5(14)	H(4b)–C(4)–H(4a)	114.1(19)
B(2)–B(5)–B(1)	59.8(2)	C(4)–B(5)–B(1)	58.0(2)
C(4)–B(5)–B(2)	104.6(2)	B(6)–B(5)–B(1)	108.8(2)
B(6)–B(5)–B(2)	59.4(2)	B(6)–B(5)–C(4)	108.4(2)
B(2)–B(6)–N(1)	115.7(2)	B(5)–B(6)–N(1)	119.3(2)
B(5)–B(6)–B(2)	58.5(2)	B(7)–B(6)–N(1)	120.2(2)
B(7)–B(6)–B(2)	58.0(2)	B(7)–B(6)–B(5)	105.6(2)
B(3)–B(7)–B(2)	60.2(2)	B(6)–B(7)–B(2)	57.7(2)
B(6)–B(7)–B(3)	107.8(2)	B(8)–B(7)–B(2)	107.4(2)
B(8)–B(7)–B(3)	55.6(2)	B(8)–B(7)–B(6)	116.4(2)
H(78)–B(7)–B(2)	126.6(10)	H(78)–B(7)–B(3)	94.3(10)
H(78)–B(7)–B(6)	94.8(9)	H(78)–B(7)–B(8)	40.8(8)
H(78)–B(7)–H(7)	109.4(14)		
B(7)–B(8)–B(3)	61.7(2)	B(9)–B(8)–B(3)	61.7(2)
B(9)–B(8)–B(7)	104.5(2)	H(78)–B(8)–B(3)	105.6(10)
H(78)–B(8)–B(7)	46.6(9)	H(78)–B(8)–B(9)	116.3(10)
H(78)–B(8)–H(8)	117.3(15)	H(89)–B(8)–B(3)	109.0(10)
H(89)–B(8)–B(7)	119.6(10)	H(89)–B(8)–B(9)	49.1(9)
H(89)–B(8)–H(8)	112.4(15)	H(89)–B(8)–H(78)	92.3(14)
B(3)–B(9)–B(1)	59.2(2)	C(4)–B(9)–B(1)	56.6(2)
C(4)–B(9)–B(3)	106.0(2)	B(8)–B(9)–B(1)	108.0(2)
B(8)–B(9)–B(3)	56.0(2)	B(8)–B(9)–C(4)	118.3(2)
H(89)–B(9)–B(1)	130.7(8)	H(89)–B(9)–B(3)	94.5(9)
H(89)–B(9)–C(4)	100.8(9)	H(89)–B(9)–B(8)	39.9(8)
H(89)–B(9)–H(9)	107.7(14)		
B(8)–H(78)–B(7)	92.6(14)	B(9)–H(89)–B(8)	91.0(13)

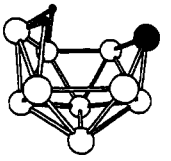

8

X-ray Structure Determination on 4c. Good-quality single crystals of **4c** were obtained, and the crystal structure has been determined. Structure solution and refinement proved to be straightforward and gave a well-defined cluster with no observable disorder. The cluster carbon atom was unambiguously assigned on the basis of intercluster bond distances, and the positions of the bridging and *endo*-terminal cluster hydrogen atoms were readily located on a Fourier difference map. Non-hydrogen and cluster hydrogen atomic coordinates and (equivalent) isotropic thermal parameters are listed in Table 5. Selected interatomic distances are in Table 6, and angles between interatomic vectors

(25) Baše, K.; Štíbr, B.; Dolanský, J.; Duben, J. *Collect. Czech. Chem. Commun.* **1981**, *46*, 2479.

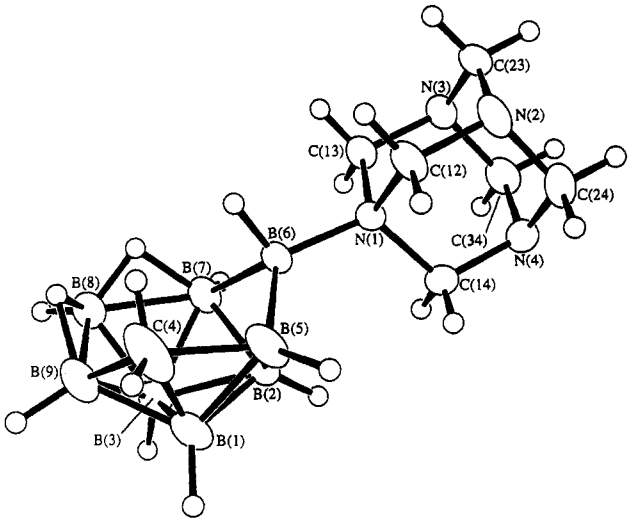

Figure 6. ORTEP drawing of the crystal and molecular structure of *exo*-6-(uro)-*arachno*-4-CB_8H_{12} (**4c**).

are in Table 7. An ORTEP[26] diagram of the molecular structure of **4c** is shown in Figure 6 and is in full agreement with the NMR data (see Tables 3 and 4) and the general structure **4** in Scheme 1 to demonstrate that the crystal was representative of the bulk sample. The crystallographic study confirms the gross similarity of the molecule to that of the isoelectronic and isostructural dicarbaborane *arachno*-4,6-$C_2B_7H_{13}$ (**7**), for which the basic molecular structure has been determined previously on its 4,6-Me_2 derivative.[27] A notional subrogation of one of the two {CH_2} vertices in structure **7** by the isoelectrolobal {BHL} unit directly leads to structure **4**. The molecule of **4c** is based on a nine-vertex *arachno* structural motif,[5,28] with two bridging hydrogens and the {CH_2} and {BHL} (L = uro) units in two "projecting", low-coordinate positions[28] of the open hexagonal face. The two B(7)–H–B(8) and B(8)–H–B(9) hydrogen bridges are asymmetrical, with shorter B–μ-H distances flanking the {B(8)} vertex, as are adequate distances in Me_2-**7**.[27] A general comparison of the other equivalent B–B and C–B distances in Me_2-**7** and **4c** in fact indicates a marked agreement between both of these structures, the maximum differences being in the range of *ca.* 2.5 pm.

Conclusions

The twelve-vertex [*nido*-7,9-$C_2B_{10}H_{13}$]$^-$ anion is readily synthesized from the commercially available dicarbaborane *closo*-1,2-$C_2B_{10}H_{12}$.[8,9] The cluster degradation reactions involving loss of one {CH} vertex that are outlined in this paper, therefore, indicate interesting new possibilities and approaches for the synthesis of smaller cage monocarbaborane compounds that avoid using hazardous reagents such as sodium cyanide with decaborane.[25,29] We are currently investigating other variations of this general cluster degradation process that involves the loss of one {CH} vertex from the twelve-vertex dicarbaborane cage systems, and we are thereby hoping to develop other new synthetic approaches in this area of carborane chemistry. These, together with other specific (see, for example, refs 8, 9, 25, and 30) and general[3-7] cluster degradation techniques, and allied with systematic routes for the incorporation of boron[3-7] and main-group heteroatoms[6,30,31] into these clusters, will we hope eventually result in a powerful and extensive armory for synthetic strategists in polyhedral boron-containing chemistry.

Acknowledgment. The authors thank the Czechoslovak Academy of Sciences (Grant Nos. 43203 and 432402), the Royal Society (London) (support to B.Š. and J.D.K.), the SERC (U.K.) for equipment grants, Borax Research Ltd. (Chessington, U.K.) for support, and Dr. T. S. Griffin, Dr. R. Walker, and Dr. D. M. Wagnerová for their helpful interest. We also wish to thank Dr. Z. Weidenhoffer and Mr. D. Singh for mass spectroscopic measurements and the late Dr. H. Plotová for elemental analyses.

Supplementary Material Available: Tables of crystal data, hydrogen coordinates and U values, anisotropic thermal parameters, and complete bond lengths and angles (6 pages). Ordering information is given on any current masthead page.

(26) Johnson, C. K. *ORTEPII*; Report ORNL-5138; Oak Ridge National Laboratory: Oak Ridge, TN, 1976.
(27) Voet, D.; Lipscomb, W. N. *Inorg. Chem.* **1967**, *6*, 113.
(28) (a) Williams, R. E. *Inorg. Chem.* **1971**, *10*, 210. (b) Williams, R. E. *Adv. Inorg. Chem. Radiochem.* **1976**, *18*, 67.
(29) Knoth, W. H. *Inorg. Chem.* **1971**, *10*, 598.
(30) Wegner, P. A. In *Boron Hydride Chemistry*; Muetterties, E. L., Ed.; Academic: New York, 1975; Chapter 12, pp 431–480.
(31) Todd, L. J. In *Metal Interactions with Boron Clusters*; Grimes, R. N., Ed.; Plenum: New York, 1982; Chapter 4, pp 145–171 and references therein.